

Blends of Poly(d,l-lactide) with Polyhedral Oligomeric Silsesquioxanes-Based Biodegradable Polyester: Synthesis, Morphology, Miscibility, and Mechanical Property

Tianqiang Wang, Jing Ding, Jiamin Li, Yu Liu, Jianyuan Hao

State Key Lab of Electronic Films and Integrated Devices, School of Microelectronics and Solid State Electronics, University of Electronic Science and Technology of China, Chengdu 610054, Sichuan, People's Republic of China

Correspondence to: J. Hao (E-mail: jyhao@uestc.edu.cn)

ABSTRACT: A highly branched hybrid copolymer based on polyhedral oligomeric silsesquioxane (POSS) was designed to improve the brittleness of poly(d,l-lactide) (PDLLA). The toughening material was synthesized using POSS-OH as the core, which initiated the ring-opening polymerization of ϵ -caprolactone and d,l-lactide sequentially to form the highly branched POSS-*g*-poly(ϵ -caprolactone)-*b*-poly(d,l-lactide) (POSS-*g*-PCL-*b*-PLA) copolymer with eight PCL-*b*-PLA arms. The POSS-*g*-PCL-*b*-PLA copolymer had a very good dispersion in the PDLLA matrix with the size of microdomains smaller than 1 μm when added at a low content below 10 wt %. In related to the nano-scale size of microdomains in the blends, the crystallinity of PCL blocks was significantly suppressed. Thus, the addition of POSS-*g*-PCL-*b*-PLA is very effective to improve the roughness of the matrix polymer when added at a low content. © 2014 Wiley Periodicals, Inc. *J. Appl. Polym. Sci.* **2014**, *131*, 40776.

KEYWORDS: biocompatibility; biodegradable; biomaterials; blends; composites

Received 29 December 2013; accepted 27 March 2014

DOI: 10.1002/app.40776

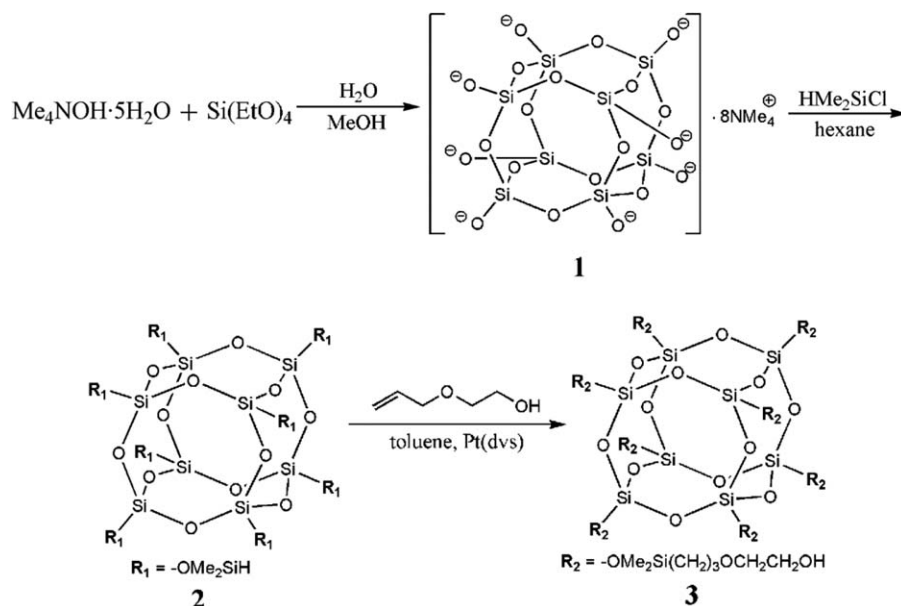
INTRODUCTION

Poly(lactic acid) (PLA) has been very attractive to tissue engineering scaffold because of their high strength, modulus, transparency and controllable biodegradability, and the safety of their degraded products. However, the inherent brittleness of PLA is one of the disadvantages that restrict its applications.^{1,2} Therefore, in many applications, PLA needs to be plasticized. Some methods, such as copolymerization with other monomers, plasticization and blending with other biodegradable flexible polymers (Polyethylene glycol or PCL), have been successfully used to obtain the desired mechanical properties of PLA.^{3–6} However, one of the most important drawbacks of these methods is the sharp reduction in strength and modulus of the materials.

Polyhedral oligomeric silsesquioxanes (POSS) have attracted more and more attention recently because of their hybrid inorganic–organic nature as nanomaterials.^{7,8} As is well known, most POSS molecules are characterized by a peculiar cage structure, the inorganic core of the cage may provide molecular reinforcement, whereas the organic groups may increase compatibility with polymers. The chemistry of POSS is quite flexible, and it can be easily altered by chemically altering the substituent groups. The usage of POSS was enlarged through altering the groups. POSS molecules can be incorporated into

polymers through polymerization or direct blending to prepare the polymer nanocomposites.^{9–13} Some properties of the polymer nanocomposites, such as heat distortion, melt strength, moduli, oxidation resistance, and permeability to gases, have been improved significantly. A majority of polymers blended with POSS have been reported, among these studies most of them are traditional polymers such as polyethylene, polypropylene, poly(methyl methacrylate), poly(methylvinylsiloxane) elastomers, and polyimide.^{14–19}

In recent years, PLA/POSS nanocomposites have been studied to improve the mechanical properties of PLA.^{20–29} There are two kinds of ways: (1) POSS is incorporated into the polymer through direct blending. It has been reported that PLLA/POSS nanocomposites have enhanced crystallization rate, improved mechanical properties, and accelerated hydrolytic degradation when compared with pristine PLLA.²⁶ However, for this method, obtaining a fine and stable dispersion of POSS molecules within the polymers is an important issue, which depends on the interactions between POSS substituent groups and the polymers. At the same time, using pure POSS could not effectively improve the brittleness of (PLA). (2) By blending synthesized core–shell particles and PLLA, the resulting fully biodegradable nanocomposites will exhibit an increase in elongation at break while maximum maintaining other mechanical

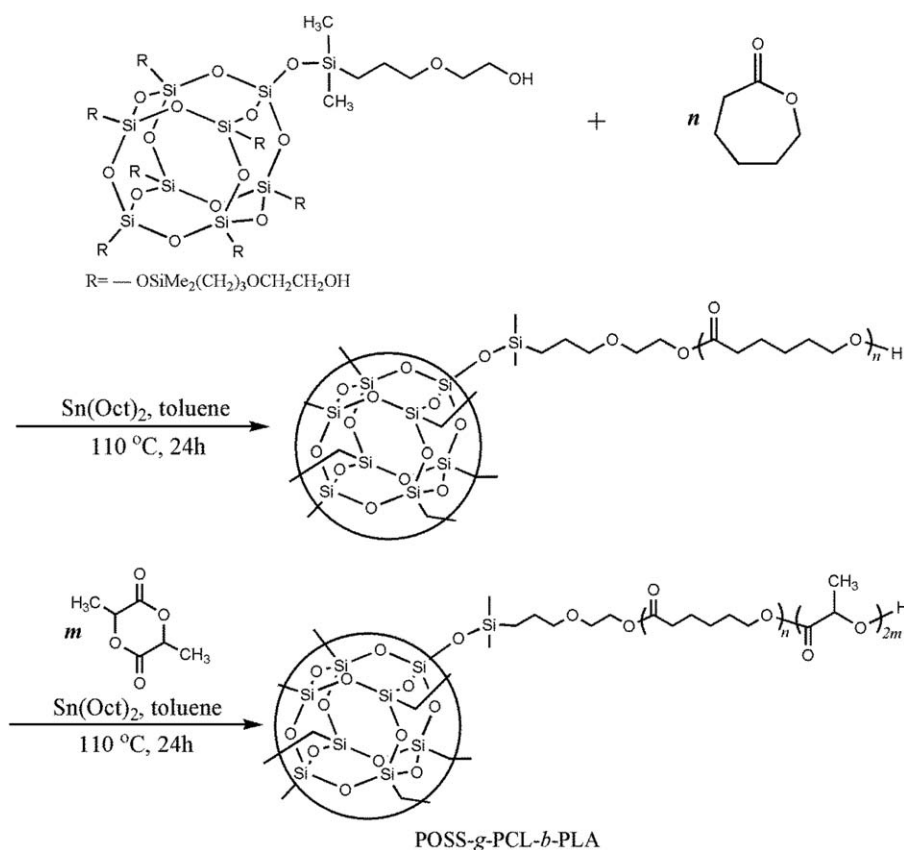


Scheme 1. Synthetic method for the preparation of POSS-OH.

properties. The shell polymers also can improve the compatibility with PLLA. poly(ϵ -caprolactone-co-lactide)PCLLA-POSS hybrids were synthesized via the ring-opening polymerization of L-lactide and ϵ -caprolactone with POSS. Then, PLLA/PCLLA-POSS nanocomposites were made by blending PLLA with PCLLA-POSS hybrids in solution and had exhibited improved

brittleness property and maintained high modulus and tensile strength of PLA.²⁸

In this study, we have designed and synthesized a highly branched POSS-containing copolymer (POSS-*g*-PCL-*b*-PLA) with a core-shell-corona structure to improve the toughness of the PDLLA matrix polymer. The toughening copolymer



Scheme 2. Synthetic method for the preparation of POSS-*g*-PCL-*b*-PLA.

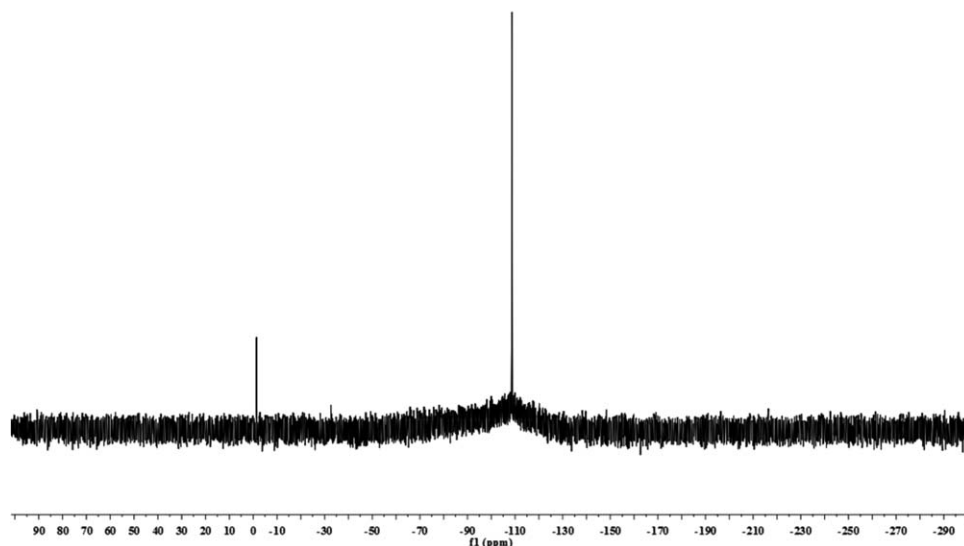


Figure 1. ^{29}Si NMR spectrum of POSS-H in CDCl_3 .

composes of one POSS core and eight PCL-PLA block copolymer arms, in which the flexible PCL blocks forms the shell region and the hard PLA blocks forms the corona area. The highly branched feature of POSS-*g*-PCL-*b*-PLA allows its good dispersion in the PDLA matrix, and very effective toughening effect is achieved when it is added at a low content.

EXPERIMENTAL

Materials

CL (Aldrich, 99%) was dried over CaH_2 at room temperature for 48 h and distilled under reduced pressure. D,L-LA was synthesized from d,l-lactic acid and purified by repeated recrystallization from distilled ethyl acetate until a mole percent purity of at least 99.9% was obtained. The ROP catalyst, tin (II) ethyl hexanoate ($\text{Sn}(\text{Oct})_2$; Aldrich) was degassed before use. PDLA ($M_n = 100000$) was synthesized through ring-opening polymerization of d, l-lactide using $\text{Sn}(\text{Oct})_2$ as catalyst in our lab. Other reagents were used as received.

Synthesis of a Highly Branched POSS-OH

POSS-OH was prepared with the method described in the literature,^{30,31} and the synthesis process has been showed in Scheme 1. The cage-like octakis(dimethylsiloxy)silsesquioxane (2) was synthesized via the one pot method, in which the tetramethylammonium silicate octamer was prepared at first by the hydrolysis and polycondensation of tetraethoxysilane with the aqueous tetramethylammonium hydroxide (1) and then the tetramethylammonium silicate octamer was silanized by dimethylchlorosilane to give the product POSS-H (2). And then reaction of (2) with 2-allyloxyethanol using platinum divinyltetramethyldisiloxane complex [$\text{Pt}(\text{dvs})$] as catalyst to produce POSS-OH (3).

Synthesis of POSS-*g*-PCL-*b*-PLA Hybrid Nanomaterials

The polymerization was processed in a glass flask under stirring at 110°C (oil bath). This flask was equipped with a three way stopcock and was previously flame dried and purged with nitrogen. First, it was charged with 0.05 g POSS-OH, 10 mL dry toluene, 2.0 g ϵ -CL, and 0.02 g $\text{Sn}(\text{Oct})_2$. The mixture was heated

to 110°C and the polymerization was left to proceed for 24 h. Then 2.0 g d, l-LA and 0.04 g $\text{Sn}(\text{Oct})_2$ were added in the mixture with the protection of nitrogen. Another 24 h was also needed to finish the polymerization (Scheme 2). After polymerization, the result product was finally purified twice by dissolving into chloroform and then precipitated in a 10-folds excess of ethanol. The purified copolymers were dried under vacuum at 60°C for 48 h.

Preparation of Blends of PDLA and POSS-*g*-PCL-*b*-PLA Thin Films

The PDLA films containing 0%(PDLA), 2%(PDLA-2), 5%(PDLA-5), 10%(PDLA-10), and 20%(PDLA-20) POSS-*g*-PCL-*b*-PLA were processed by casting solutions of the PDLA and POSS-*g*-PCL-*b*-PLA in chloroform onto the surfaces of aluminum foil. The films were dried at 60°C under atmospheric pressure for 24 h and then further dried under vacuum at room temperature for another 24 h. The final polymer films with

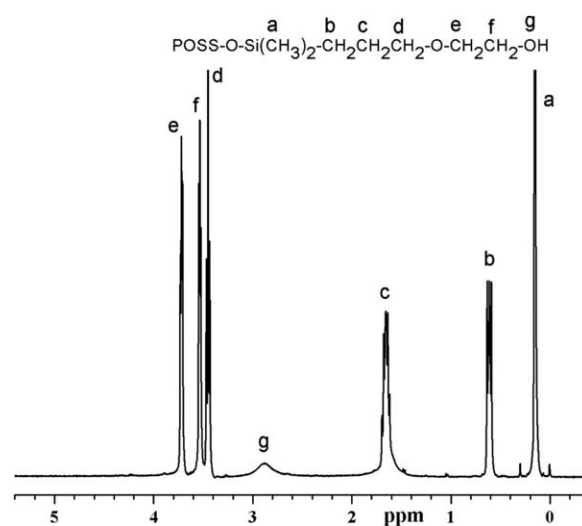


Figure 2. ^1H NMR spectrum of POSS-OH in CDCl_3 .

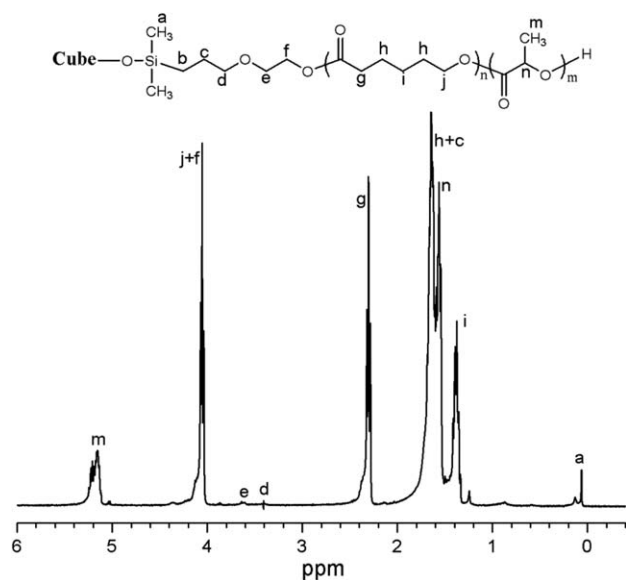


Figure 3. ^1H NMR spectrum for POSS-g-PCL-b-PLA.

thicknesses of 0.2–0.4 mm were cut into rectangle shape for further test.

Methods

The ^1H -NMR and ^{29}Si -NMR spectra were recorded on a 300 MHz ^1H -NMR spectrometer (Bruker AV-300), using tetramethylsilane as an internal reference and CDCl_3 as the solvent.

The gel permeation chromatography (GPC) measurements were performed on a Waters 1515 GPC system with a Waters 2414 refractive-index detector (America) using THF as eluent and polystyrene as standards.

Microscopic images of particles were obtained from scanning electron microscope (SEM, FEI INSPECTF) and measured at 10 kV after coated with a thin layer of sputtered gold.

The crystal structure of the film was characterized by X-ray diffraction (XRD, BEDE D1) using $\text{CuK}\alpha$ radiation in the mode of θ - 2θ scan.

DSC analysis was performed on a Phoenix 204 DSC system to study the thermal properties of the synthesized copolymers. The samples were first heated to 80°C and kept at this temperature for 5 min to eliminate the thermal history. The cooling curves were recorded when the samples were cooled from 80°C to 30°C at a nominal rate of $10^\circ\text{C}/\text{min}$. After keeping the samples at 30°C for 5 min, the heating curves were recorded when they were heated from 30 to 80°C at a nominal rate of $10^\circ\text{C}/\text{min}$.

The tensile tests were performed on a SANS Testing Machine at a cross-head speed of 10 mm/min at room temperature (25°C). Rectangular shapes ($5 \times 40 \text{ mm}^2$, $N=5$) were cut from the films for tensile testing. The mechanical data were calculated from the stress-strain curves of each sample.

Izod impact tests were performed at room temperature with an instrument XBJ-7.5/11. The specimens (80 mm long, 10 mm thick, and 4 mm wide) were prepared in a hot press at 180°C for 15 min under load.

RESULT AND DISCUSSION

Synthesis of a Highly Branched POSS-OH

The spectrum of ^{29}Si NMR for POSS-H shows a peak with the maximum around -110.0 ppm ($\text{Si}(\text{OSi})_4$), which indicates that the chemical environment around Si atoms is about the same (Figure 1). It is concluded that caged silsesquioxane structure of POSS-H is indeed formed. At the same time, the peak appeared nearby -2.0 ppm , which means $\text{Si}(\text{CH}_3)_2\text{H}$. This phenomenon is in agreement with the literature. And the structure of POSS-OH was confirmed by ^1H NMR spectroscopy, which is shown in Figure 2. The peak signals at different ppm have been assigned to the hydrogen of the POSS-OH, the peak appears within 2.8–3.0 ppm is the group of OH, and the intensity of this peak is about one-sixth to the peak at 0.15 ppm, which represents $(\text{CH}_3)_2$. Therefore in terms of probability, the POSS-OH has caged-like structure and is composed of eight $-\text{OH}$ groups.

POSS-g-PCL-b-PLA Hybrid Nanomaterials Studies

The POSS-g-PCL-b-PLA hybrid nanomaterial was synthesized through two-step method, which is shown in Scheme 2. The first step was ring-opening polymerization of CL using POSS-OH as initiator; the second step was ring-opening polymerization of d,l-LA using the POSS-PCL-OH as initiator. The resultant product was determined by ^1H NMR spectroscopy (Figure 3). It can be seen from the spectroscopy that the peak at 2.88 (δH) ppm which belongs to the $-\text{OH}$ of POSS-OH did not show up, which means completely reacted to initiate CL. The peaks observed at 4.05 (δH^j), 2.30 and 1.65 (δH^h), 1.38 (δH^i) ppm are attributed to $-\text{CH}_2-$ of PCL chains. The existence of PLA segments can be identified by the chemical shifts at 5.17 (δH^m) and 1.56 (δH^n) ppm, which were attributed to the resonances of $-\text{CH}_3$ and $-\text{CH}$ of PLA, respectively. The peaks observed at 3.61 (δH^e), 3.41 (δH^d), 1.65 (δH^c), and 0.06 (δH^a) are attributed to $-\text{CH}_2-$ of POSS-OH. It demonstrated that the product really is composed of POSS, PLA, and PCL segments. At the same time, there is no peak around 2.30 which indicated that no ester exchange reaction between PCL and PLA. It confirmed PCL and PLA were in the form of block copolymer.

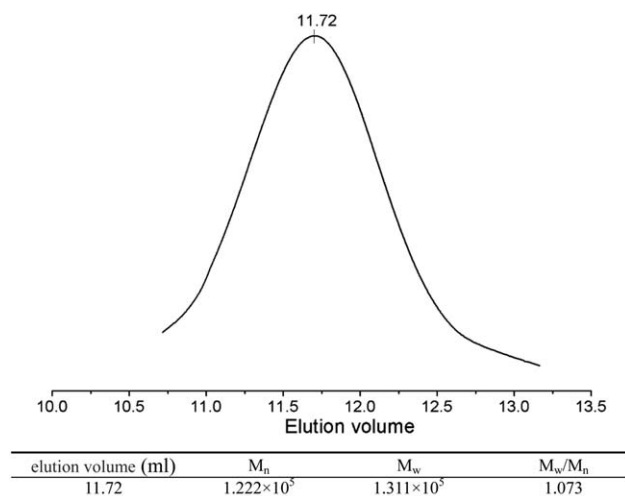


Figure 4. GPC trace for POSS-g-PCL-b-PLA.

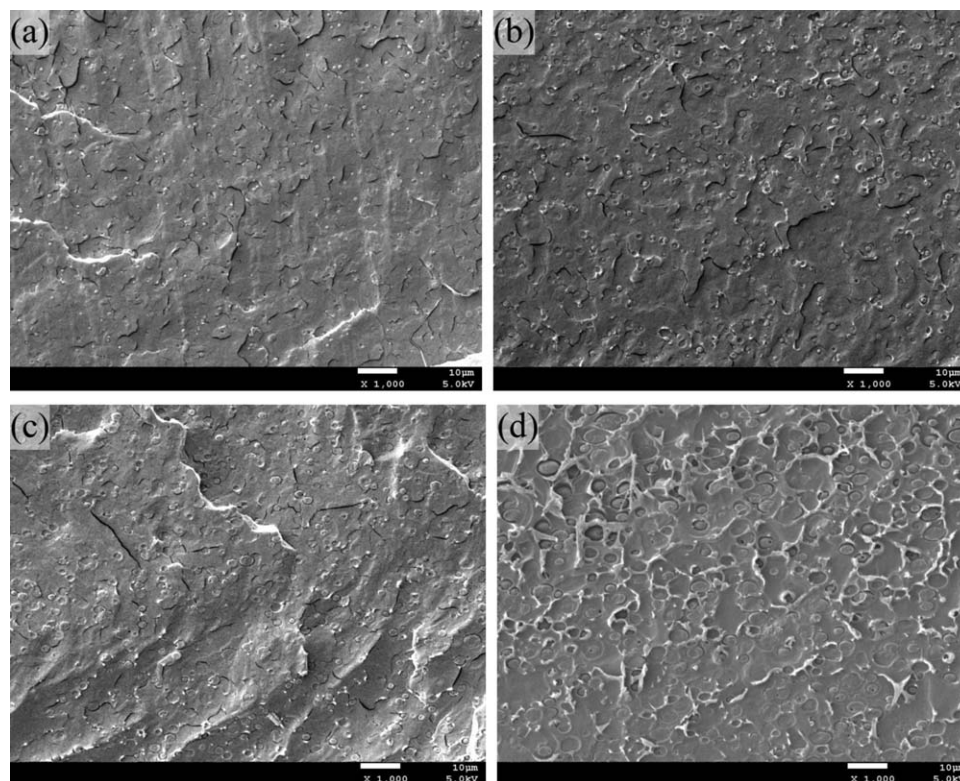


Figure 5. SEM image of fracture surface of PDLLA-2, PDLLA-5, PDLLA-10, and PDLLA-20.

The molecular weights and molecular weight distributions were also tested using GPC. In Figure 4, a single smooth signal caused by the product occurs at 11.72 min of elution time. There is no evidence to indicate that the products contained any PLA or PCL homopolymeric fractions or PCL-*b*-PLA copolymer. The molecular weight of the product was 1,20,000 and the molecular weight distribution was 1.073. Therefore, the structure of POSS-*g*-PCL-*b*-PLA was successfully tested by simple ^1H NMR and GPC methods.

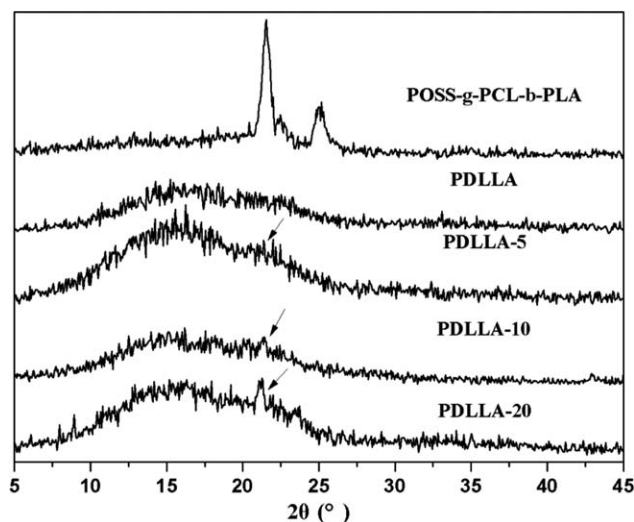


Figure 6. XRD patterns of POSS-*g*-PCL-*b*-PLA, PDLLA, PDLLA-5, PDLLA-10, and PDLLA-20 composites.

Dispersion of POSS-*g*-PCL-*b*-PLA in the PDLLA Matrix

Figure 5 show the liquid nitrogen fracture surfaces of the PDLLA films with different contents of POSS-*g*-PCL-*b*-PLA. The magnification of the pictures is 1000. From Figure 5(a), homogeneous distribution of micro-domains with the size of $0.3\ \mu\text{m}$ appeared when 2 wt % POSS-*g*-PCL-*b*-PLA was added. The size of microdomains increased with an increase of POSS-*g*-PCL-*b*-PLA content, but the toughening copolymer still had very good dispersion in the PDLLA matrix for the films with POSS-*g*-PCL-*b*-PLA content below 10 wt % [Figure 5(a–c)]. Because the PLA and PCL blocks are very immiscible, this good

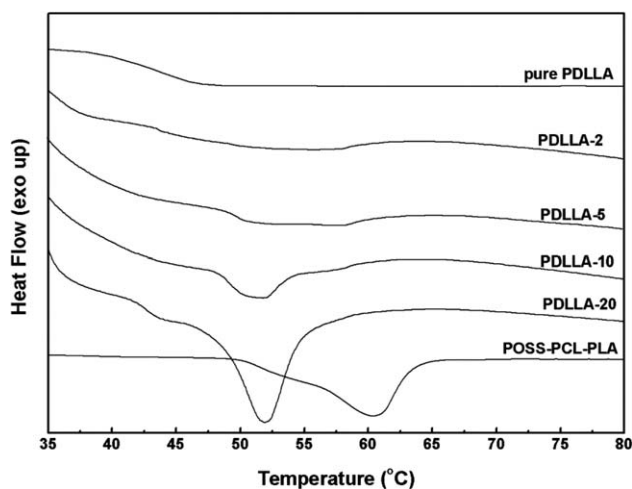


Figure 7. DSC heating scans of the samples.

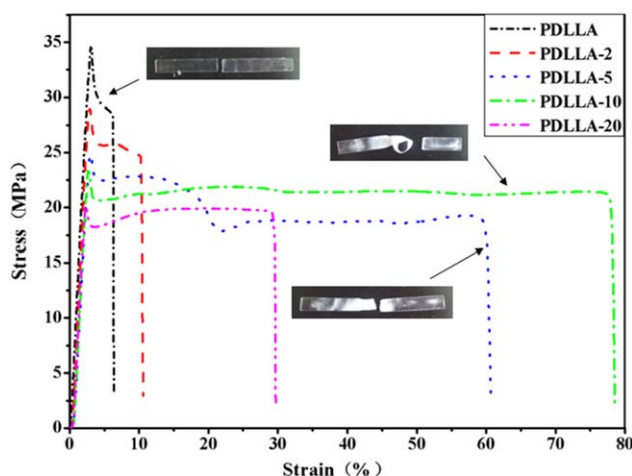


Figure 8. Stress–strain curves and tensile fracture surfaces of the samples. [Color figure can be viewed in the online issue, which is available at wileyonlinelibrary.com.]

dispersion was partially related to the PCL-PLA block nature. Additionally, the rigid highly branched structure of POSS-g-PCL-*b*-PLA copolymer was also presumed to play an important role for the nano-scale size of microdomains and good miscibility of the blends. The corona PLA blocks surrounded the internal PCL blocks, decreasing the tendency of mixing and agglomeration of the POSS-g-PCL-*b*-PLA molecules.

XRD Analysis of PDLLA with Different POSS-g-PCL-*b*-PLA Contents

Figure 6 illustrates the XRD patterns of POSS-g-PCL-*b*-PLA and different samples. It is seen from the patterns that POSS-g-PCL-*b*-PLA showed characteristic peak at around 21.8° and 24.6° for PCL.³² However, the characteristic diffraction peaks of POSS at around 7.89° and 8.77° did not show up. After polymerization, POSS was confined in the core of the POSS-g-PCL-*b*-PLA, and the content of POSS was very low compared with the PCL and PLA segments. Therefore, the characteristic diffraction peaks of POSS are very hard to be detected compared with PCL segment.

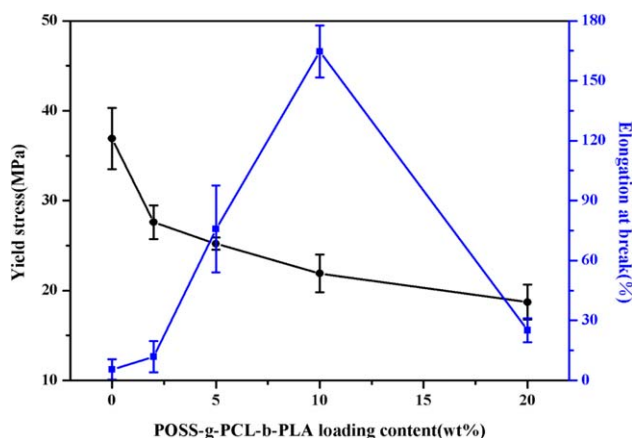


Figure 9. Mechanical properties of PDLLA composites: change of yield stress and elongation at break with blend composition. [Color figure can be viewed in the online issue, which is available at wileyonlinelibrary.com.]

As we all know that PDLLA is amorphous polymer, there are no characteristic diffraction peaks for amorphous polymer, so dispersion of POSS-g-PCL-*b*-PLA in the PDLLA also can be clarified through this method. As the content of POSS-g-PCL-*b*-PLA increased to 10%, the peaks at around 21.8° and 24.6° showed up, and when increased to 20%, the intensity of peaks got stronger. When the content of POSS-g-PCL-*b*-PLA is lower than 10%, the characteristic diffraction peaks of PCL can not be found from the patterns. The appearance of the diffraction peaks of POSS-g-PCL-*b*-PLA in the PDLLA-10 and PDLLA-20 nanocomposites may be related to the fact that the agglomeration and crystallization of POSS-g-PCL-*b*-PLA particles are easier at higher concentration. However, no clear characteristic peaks are found for PDLLA-2 and PDLLA-5 nanocomposites probably due to the low POSS-g-PCL-*b*-PLA contents. And when the concentration of POSS-g-PCL-*b*-PLA is low, the distribution in PDLLA matrix may be also very good.

Thermal Analysis of PDLLA with Different POSS-g-PCL-*b*-PLA Contents

A series of PDLLA polymers with different contents of POSS-g-PCL-*b*-PLA were analyzed by DSC. The DSC second heating curves (performed at $10^\circ\text{C}/\text{min}$) of the nanocomposites are shown in Figure 7. The POSS-g-PCL-*b*-PLA exhibits a melting peak at about 60°C , which is corresponding to the PCL segment. When the content of POSS-g-PCL-*b*-PLA is lower than 10% in PDLLA matrix, there are no melting peak appeared. However, when the content reaches 10% or higher, melting peak at 54°C appeared, and the intensity of the peak gets stronger as the POSS-g-PCL-*b*-PLA content increased. This phenomenon is related to the distribution of POSS-g-PCL-*b*-PLA in PDLLA matrix. As the content of POSS-g-PCL-*b*-PLA is low, they dispersed in the PDLLA matrix in the form of single molecule. The PCL segment was confined in micro-space (several nanometers) by the rigid chain of PDLLA. And because of pinning of POSS core, the PCL segment can not move freely to crystallize. As more POSS-g-PCL-*b*-PLA added in the polymer matrix, the distance among POSS-g-PCL-*b*-PLA molecules are much closer, they tend to aggregate with each other. PLA segments can not prevent the aggregation of the PCL segments from different POSS-g-PCL-*b*-PLA molecules, and micro phase appeared in the polymer matrix. Thus POSS-g-PCL-*b*-PLA showed crystallization capacity gradually when the content of POSS-g-PCL-*b*-PLA increased in the polymer matrix.

Mechanical Properties of the Hybrid Materials

The mechanical properties of the polymer composites were investigated by tensile experiments, and the typical stress–strain curves for the samples with different amounts of POSS-g-PCL-*b*-PLA are shown in Figure 8. The samples initially proceed with elastic deformation and after reaching a nontypical yield point, the stress kept constantly until the strain reaches a critical point. Beyond this point, with further increasing strain, the yield stress rapidly increases until the samples are fractured. And it also can be seen from Figure 9 that as the content of POSS-g-PCL-*b*-PLA increased in the PDLLA, the maximum yield stress decreased gradually, but the elongation at break increased obviously. It is worth noting that even the content of POSS-g-PCL-*b*-PLA is very low (5%), the toughness of the PDLLA is significantly improved. The result

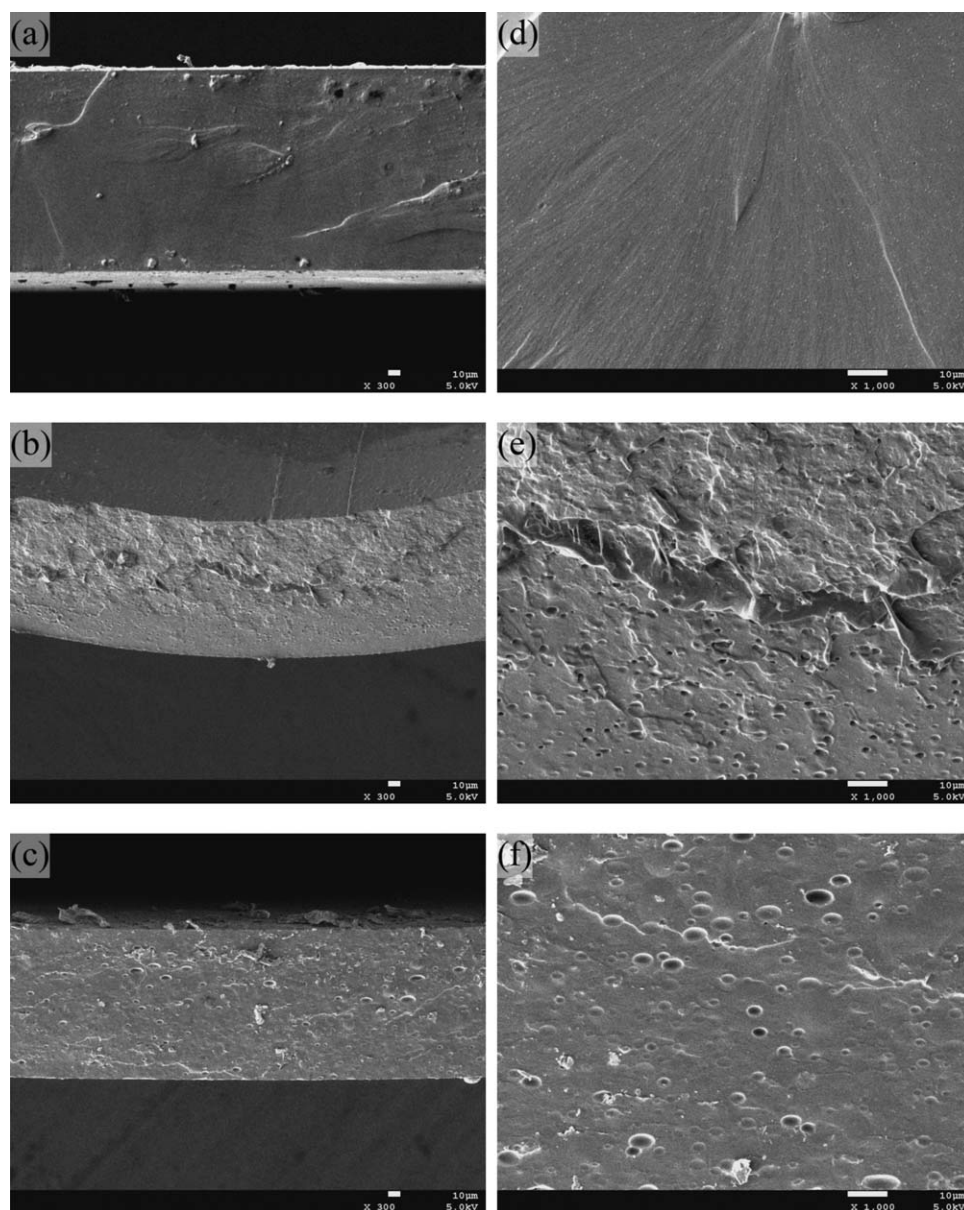


Figure 10. SEM image of fracture surface of PDLLA-5(a), PDLLA-10(b), and PDLLA-20(c). (d), (e), and (f) are the high magnification pictures of (a), (b), and (c).

indicated that the addition of POSS-*g*-PCL-*b*-PLA in PDLLA indeed increases the toughness and decreases the tensile stress of PDLLA. As we all know that PCL is a ductile polymer that is able to sustain larger deformation and also has low yield stress. Therefore, the PCL section in POSS-*g*-PCL-*b*-PLA is the real reason for the phenomenon. It is well-known and commonly admitted that the mechanical properties of polymer nanocomposites, especially the modulus, depend to a great extent on filler dispersion and interfacial interaction, and are increased only when good dispersion of the nanofiller and effective stress transfer at the polymer/filler interface are guaranteed.²⁴ In this sense, the improvements in the mechanical properties can also verify the uniform dispersion of POSS-*g*-PCL-*b*-PLA in the PDLLA matrix. We also find that as the content of POSS-*g*-PCL-*b*-PLA in PDLLA passes 20%, the elongation at break decreased sharply. In fact, more POSS-*g*-PCL-*b*-PLA

in PDLLA means more bigger aggregated POSS-*g*-PCL-*b*-PLA particles dispersing in the PDLLA. The fracture of the film happened at this region. The mechanism also can be seen in Figure 9.

Figure 10 shows the SEM images of tensile sectional morphology of PDLLA-0, PDLLA-10, and PDLLA-20. The tensile sectional morphology of pure PDLLA is very smooth and there is no any microregion of micro-phase separation in the surface. That means a typical brittle fracture. The surface of PDLLA-10 is very rough, and layer and filamentous structure were appeared, indicating a typical ductile fracture. The fracture surface of PDLLA-20 is not rougher than PDLLA-10, and there is no obvious layer and filamentous structure appeared in PDLLA-20, the process of tensile failure includes brittle fracture and ductile fracture at the same time. From figure 10e and figure

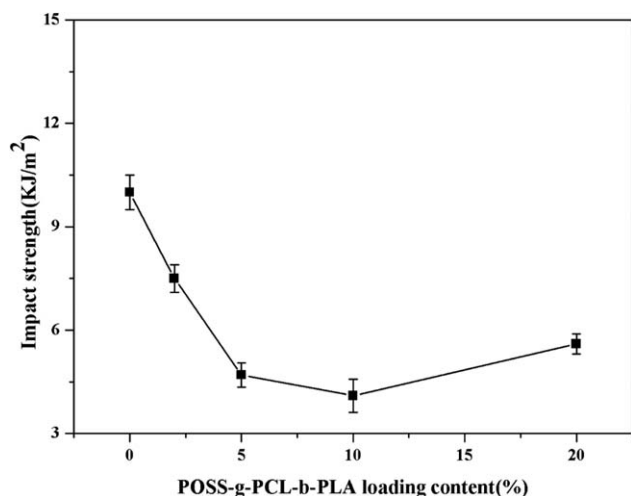


Figure 11. Effect of the incorporation of POSS-g-PCL-*b*-PLA on the impact strength of PDLLA.

10f, spherical particles (microphase separation) dispersed in the surface, and as the content of POSS-g-PCL-*b*-PLA increased, the size of the particles get bigger, resulting in the obvious decline of the maximum yield stress and the elongation at break. The aggregation of POSS-g-PCL-*b*-PLA may be the reason for microphase separation, which is also proved by XRD and DSC.

The effect of incorporation of POSS-g-PCL-*b*-PLA on the impact strength of PDLLA is shown in Figure 11. It can be seen that the impact strength of PDLLA decreased after incorporation of POSS-g-PCL-*b*-PLA, and as the content increased the impact strength did not change so much. Compared with the M_n of PDLLA (1.0×10^5), the M_n of each arm in POSS-g-PCL-*b*-PLA is only around 1.0×10^4 , it is hard for it to act as buffer material under an instantaneous force. At the same time, the size of the domain of POSS-g-PCL-*b*-PLA in PDLLA matrix is so small that it could not immediately and effectively transfer the instantaneous force.

CONCLUSIONS

POSS-g-PCL-*b*-PLA was successfully synthesized by ring-opening polymerization, and POSS-g-PCL-*b*-PLA/PDLLA nanocomposites were also prepared via solution casting method and characterized for mechanical, thermal, morphology properties. Good compatibility and distribution between POSS-g-PCL-*b*-PLA and PDLLA matrix has realized just by adding the PLA segment, however, aggregation inevitably happened. As the content of POSS-g-PCL-*b*-PLA increased, the aggregation got more serious, which affected the final mechanical property of PDLLA. The yield stress decreased and elongation at break increased as the content of POSS-g-PCL-*b*-PLA increased. That is because the core-shell structure of POSS-g-PCL-*b*-PLA, which significantly improved the toughness of the polymer matrix.

ACKNOWLEDGMENTS

This work was supported by the National Natural Sciences Fund of China (No. 30970725, No. 51273034), the Opening Project of

the State Key Laboratory of Polymer Materials Engineering (Sichuan University, KF201201).

REFERENCES

- Laura, M.; Lorenzo, D. *Eur. Polym. J.* **2005**, *41*, 569.
- Iannace, S.; Nicolais, L. *Polymer* **1997**, *38*, 4003.
- Lin, Y.; Zhang, K.Y.; Dong, Z.M.; Dong, L.S.; Li, Y.S. *Macromolecules* **2007**, *40*, 6257.
- Shibata, M.; Teramoto, N.; Inoue, Y. *Polymer* **2007**, *48*, 2768.
- Auras, R.; Harte, B.; Selke, S. *Macromol. Biosci.* **2004**, *4*, 835.
- Chigwada, G.; Jash, P.; Jiang, D.D.; Wilkie, C.A. *Polym. Degrad. Stab.* **2005**, *89*, 85.
- Kannan, R.; Salacinski, H.; Butler, P.; Seifalian, A. *Acc. Chem. Res.* **2005**, *38*, 879.
- Harrison, P. *J. Organ. Chem.* **1997**, *542*, 141.
- Guo, Q.Y.; Knight, T.P.; Wu, J.; Mather, T.P. *Macromolecules* **2010**, *43*, 4991.
- Laura, R.; Saverio, R.; Orietta, M.; Alessandro, B.; Federica, B. *Polymer* **2005**, *46*, 6810.
- Wang, D.; Fredericks, P.M.; AHaddad Hill, D.J.T.; Rasoul, F.; Whittaker, A.K. *Polym. Degrad. Stab.* **2011**, *96*, 123.
- Wang, R.Y.; Wang, S.F.; Zhang, Y. *J. Appl. Polym. Sci.* **2009**, *113*, 3095.
- Ni, Y.; Zheng, S.X. *Macromolecules* **2007**, *40*, 7009.
- Fina, A.; Tabuani, D.; Frache, A.; Camino, G. *Polymer* **2005**, *46*, 7855.
- Lee, Y.; Huang, J.; Kuo, S.; Chang, F. *Polymer* **2005**, *46*, 10056.
- Zhao, Y.; Schiraldi, D. *Polymer* **2005**, *46*, 11640.
- Sharon, Y.; Cohen, R.; Boyce, M. *Polymer* **2007**, *48*, 1410.
- Zhang, Y.; Lee, S.; Yoonessi, M.; Liang, K.; Pittman, C. *Polymer* **2006**, *47*, 2984.
- Kopesky, E.; McKinley, G.; Cohen, R. *Polymer* **2006**, *47*, 299.
- Pan, H. Master Dissertation, Preparation and Properties of PLA/POSS Nanocomposites Beijing University of Chemical Technology, Beijing, **2010**.
- Pan, H.; Qiu, Z.B. *Macromolecules* **2010**, *43*, 1499.
- Yu, J.; Qiu, Z.B. *Thermochim. Acta.* **2011**, *519*, 90.
- Kodal, M.; Sirin, H.; Ozkoc, G. *Polym. Eng. Sci.* **2014**, *54*, 264.
- Quang, V.B.; Jiyeon, C.; Yoon, K.J.; Bang, J.P.; Dong, K.H. *Macromol. Res.* **2012**, *20*, 996.
- Yu, J.; Qiu, Z.B. *ACS Appl. Mater. Interfaces* **2011**, *3*, 890.
- Qiu, Z.B.; Pan, H. *Compos. Sci. Technol.* **2010**, *70*, 1089.
- Zhang, X.J.; Sun, J.S.; Fang, S.M.; Han, X.N.; Li, Y.D.; Zhang, C.G. *J. Appl. Polym. Sci.* **2011**, *122*, 296.
- Sun, Y.; He, C.B. *Macromolecules* **2013**, *46*, 9625.
- Lee, J.H.; Jeong, Y.G. *J. Appl. Polym. Sci.* **2010**, *115*, 1039.
- Zou, J.; Chen, X.; Jiang, X.B.; Zhang, J.; Guo, Y.B.; Huang, F.R. *Exp. Polym. Lett.* **2011**, *8*, 662.
- Zhang, C.X.; Laine, R.M. *J. Am. Chem. Soc.* **2000**, *122*, 6979.
- Wang, J.L.; Dong, C.M. *Polymer* **2006**, *47*, 3218.